

# Ge dots embedded in silicon dioxide using sol-gel deposition

T. F. STOICA\*, M. GARTNER<sup>a</sup>, V. S. TEODORESCU, T. STOICA

*National Institute of Materials Physics, P.O. Box Mg. 7, 76900 Bucharest, Magurele, Romania*

<sup>a</sup>*Institute of Physical Chemistry of the Romanian Academy of Sciences, Splaiul Independentei 202, 77208 Bucharest, Romania*

A versatile method, that of sol-gel deposition was used to produce  $\text{Si}_{1-x}\text{Ge}_x\text{O}_2$  films on Si substrates. Samples after annealing at different temperatures are investigated by different techniques including high-resolution transmission electron microscopy and spectral ellipsometry. It was revealed that, by annealing at high temperatures, Ge accumulates in small clusters (5-10nm) inside of the oxide layer. By ellipsometric investigations, valuable data about the temperature evolution of the composition and optical constants were obtained.

(Received July 3, 2007; accepted October 1, 2007)

*Keywords:* Silicon dioxide, Ge dots, Sol-gel deposition

## 1. Introduction

Si and Ge nanocrystals, in particular Ge dots embedded in oxide are of large interest for nanotechnology due to the compatibility of the required processes with the well-established silicon technology, for different device applications as for example floating gate memories and single electron devices [1,2]. An advantage of Ge dots embedded in oxide over Si dots is related to the smaller gap of Ge corresponding to lower energies for injected holes or electrons. Also, a large difference between the oxidation energy of Ge and Si, leads to an easy segregation of Ge at bottom and top interfaces of the oxide [3], as well as to form clusters in a  $\text{SiO}_2$  matrix [2]. Ge dots embedded in  $\text{SiO}_2$  have been obtained using different deposition methods, as for example: d.c. magnetron sputtering [4,5], electron-beam evaporation [6], epitaxial Ge islands on subnanometer thick oxide films [7], the germanosilicate or selectively deposited on nanometer scale areas [8]. Besides nano-dot application studies, Si-Ge oxide films are studied due to the ability to change the refractive index by varying the composition of the germanosilicate which can be exploited in some photonic applications [9,10]. Sol-gel deposition method was intensively studied by our group for indium tin oxide layers [11] and implemented in this paper for SiGe oxide.

In this paper we report on Ge dots formed in oxide matrix using sol-gel deposition of  $\text{Si}_{1-x}\text{Ge}_x\text{O}_2$  on silicon substrate. This deposition method is a flexible one and offers a precise control of the composition. The effect of the post-deposition annealing on film properties and formation of Ge nano-clusters in oxide matrix has been investigated by ellipsometry and high resolution transmission electron microscopy.

## 2. Experimental details

Solution containing  $\text{GeCl}_4$  and tetraethoxysilane (TEOS) as Ge and Si precursors was used. Ge/Si ratio in solution was 5-7%. After spin coating (1000 rpm) of Si(100) substrates at room temperature, the wafers were dried for 15 min at 120°C and annealed in  $\text{N}_2$  atmosphere for 1 h at 550 °C, for complete the removal of solvents and the film  $\text{Si}_{1-x}\text{Ge}_x\text{O}_2$  formation. The grown samples were subsequently annealed at higher temperature by rapid thermal annealing (RTA) in Ar atmosphere, for 5min. at 800 °C and 950 °C.

The morphology and internal structure of the films were studied by XTEM (Cross-Section Transmission Electron Microscopy - high-resolution electron microscope Topcon 002B), SEM (Scanning Electron Microscopy) and AFM (Atomic Force Microscopy). Spectroellipsometric (SE) measurements carried out with a null ellipsometer at an incidence angle of 70° in wavelength range 370-700 nm have been modelled using Bruggemann Effective Medium Approximation (BEMA) in order to evaluate film parameters for different annealing temperatures.

## 3. Results and discussions

### 3.1 Morphology and internal structure of the film

Smooth  $\text{Si}_{1-x}\text{Ge}_x\text{O}_2$  films were obtained by sol gel deposition. A roughness of 1nm was measured by AFM on  $10 \times 10 \mu\text{m}$  areas. The AFM surface topography shows no peculiarity as can be seen in Fig. 1a. No peel off of the films at cutting edges was observed in high-magnification interference optical images (not shown here), revealing a good adherence to Si substrates. Side view SEM image

shows also a smooth top surface (Fig. 1b). A thickness value of about 110 nm can be evaluated from SEM image. However, low magnification optical microscopy show smooth fluctuations of the film thickness, perhaps due to non-uniform spin coating procedure. Also a columnar-like structure is observed in sectioned films (Fig. 1b), but this was not revealed by XTEM (Fig. 2a), which show a high homogeneity of the oxide film in low magnification images.

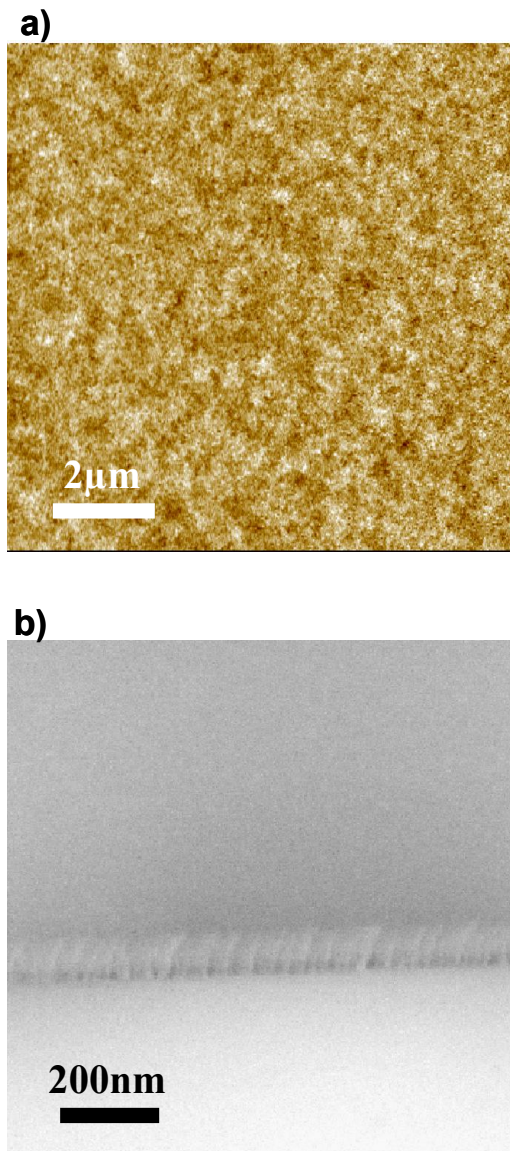


Fig. 1. Morphology images of as-grown  $\text{Si}_{1-x}\text{Ge}_x\text{O}_2$  films: a)- AFM and b)- SEM.

The top surface is relatively smooth as shown by XTEM image in Fig. 2a, but some particles of unknown origin, included in the glue are observed. A value of about 120 nm can be evaluated for the thickness of the  $\text{Si}_{1-x}\text{Ge}_x\text{O}_2$  film in Fig. 2a. At the bottom of the  $\text{Si}_{1-x}\text{Ge}_x\text{O}_2$  layer, a thin “native”  $\text{SiO}_2$  layer of 2-3 nm can be seen.

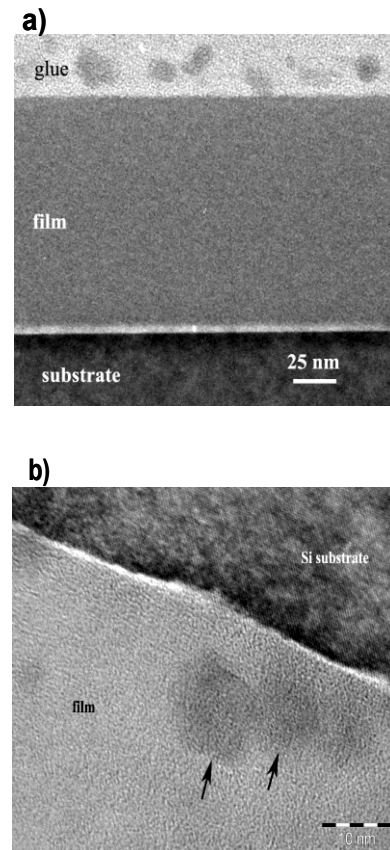


Fig. 2. a) low- and b) high- resolution XTEM images of  $\text{Si}_{1-x}\text{Ge}_x\text{O}_y$  films annealed at 950 °C.

High resolution XTEM shows the presence of dots of 5-10 nm diameter, as illustrate by the image in Fig. 2b of a sample annealed at 950 °C. These dots embedded in oxide film can be assigned to Ge clusters formed by segregation of Ge during the high-temperature annealing. As already discussed Ge segregation in  $\text{SiO}_2$  matrix has the origin in the large difference of Si-O and Ge-O energies. For long time and/or high temperature annealing, segregation of Ge as accumulations on both top and bottom interfaces of the oxide film is expected [3], but also as dots embedded in oxide [2,8]. Unfortunately, the dots observed in high temperature annealed sample show an amorphous structure. More XTEM investigations on samples obtained by an optimised annealing at intermediary temperatures will be necessary.

### 3.2 Composition and optical properties of the film

Ellipsometric measurements were performed at fix angle 70° within UV-VIS spectral range, for samples annealed at different temperatures, but obtained from the same deposition run. The experimental SE curves of  $\tan(\Psi)$  and  $\cos(\Delta)$  are shown in Fig. 3a, b. The changes induced by RTA annealing are evidently. A software program was used for the fitting of a model with 2 layers on a Si substrate to the ellipsometric functions of the experimental SE angles  $\Psi$  and  $\Delta$ , which allow us to evaluate important parameters of the films. The model

structure, designed in agreement with TEM results, includes the following layer sequence:  $\text{Si}_{1-x}\text{Ge}_x\text{O}_y$  top layer/ native  $\text{SiO}_2$  (2nm) interface layer/ Si-substrate. The optical constants of the layers were computed based on optical constants  $\varepsilon_1$ ,  $\varepsilon_2$  of the film components, using the BEMA formula. The top layer  $\text{Si}_{1-x}\text{Ge}_x\text{O}_y$  is the studied layer, consisting in a mixture of  $\text{SiO}_2$ ,  $\text{Si}_{0.6}\text{Ge}_{0.4}\text{O}_2$ , nano-voids and amorphous germanium (a-Ge), with optical constants known from literature [9,12]. Values of the  $\text{Si}_{1-x}\text{Ge}_x\text{O}_y$  film parameters corresponding to the best fit are given in Table 1. Spectral dependences of optical constants  $n$  and  $k$  evaluated for the  $\text{Si}_{1-x}\text{Ge}_x\text{O}_y$  layer after different annealing processes are shown in Fig. 3c, d.

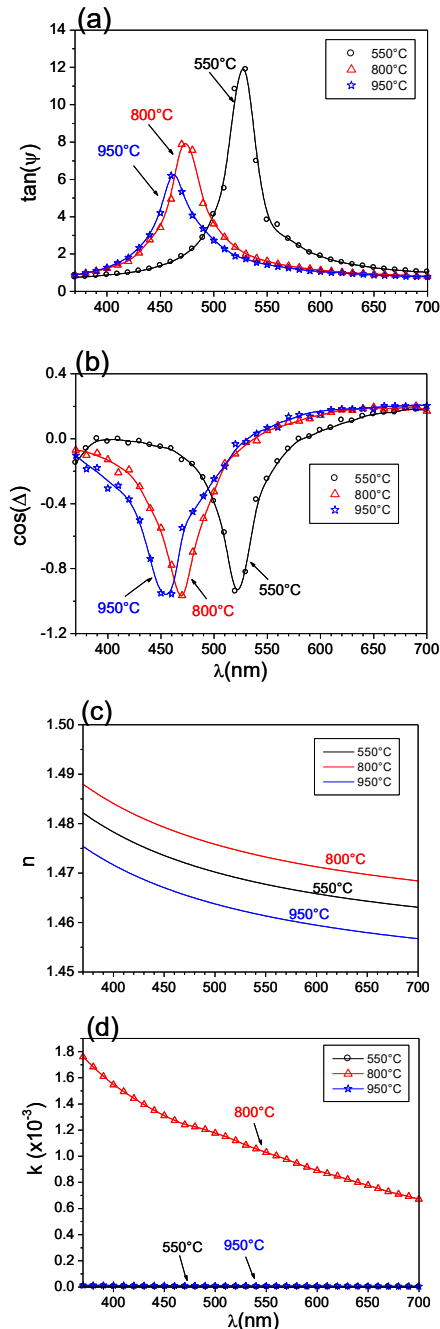


Fig. 3. a),b) Experimental SE data and c),d) refractive index  $n$  and absorption constant  $k$  for different annealing temperatures of  $\text{Si}_{1-x}\text{Ge}_x\text{O}_y$  films.

Based on modelling results of the SE analysis, we can draw some important conclusions about the annealing effects (see Table 1 and Fig. 3c, d):

1) The film thickness decreases with the annealing temperature. The effect is more pronounced between as grown sample (550° annealed) and 800° annealed one, and might be attributed to a film densification.  $\text{GeO}_2$  segregation at free top surface and its evaporation, especially at higher annealing temperature, cannot also be excluded. The film thickness of  $\sim 100$  nm is in agreement with SEM and TEM evaluation; the small difference can be attributed to film non-uniformity of different investigated areas.

2) The  $\text{GeO}_2$  concentration decreases with annealing temperature, too. The oxide is consumed for Ge cluster formation and for segregation top and down in oxide layer.

3) Segregation of Ge dots embedded in oxide is essentially observed only for moderate annealing temperature of 800°C and negligible for the rest of samples. This is consistent with the following scenario: i) At low temperature used for film formation, the Ge segregation is negligible; ii) At 800°C, a small amount of Ge ( $\sim 6\%$ ) is transformed in clusters randomly distributed in oxide film. Note that the concentration sum Ge+ $\text{GeO}_2$  at 800°C is approximately that of  $\text{GeO}_2$  in sample annealed at 550°C. It results a conservation of Ge inside the oxide layer. iii) By high-temperature annealing at 950 °C, Ge is substantially excluded from the oxide film, by segregation at top and bottom interfaces. The concentration decreases 70% relative to the initial value. The small amount of Ge clusters observed in high-resolution TEM images of 950 °C-annealed sample seems to have negligible contribution in optical constants.

4) The void density is very small for a sol-gel deposited film. It is found approximately 0.1% in samples annealed at low temperatures and increases to 0.2% by annealing at 950 °C, probable due to some low density point defects not observed in XTEM images.

5) The optical constants (Fig. 3 c,d) vary with the annealing temperature in agreement with the compositional changes in Table 1. The refractive index  $n$  is higher for sample annealed at 800 °C. The optical absorption ( $k$ -constant) is negligible for lower and higher annealing temperatures, but has a detectable value for 800 °C. These are explained by the contribution of the Ge clusters to the change of the optical constants. The reduction of the refractive index due to annealing at 950° relative to the as grown sample is associated with the decrease of  $\text{GeO}_2$  concentration in the film, while Ge clusters are negligible.

Table 1. Annealing temperature ( $T_{\text{ann}}$ ) and ellipsometric fitting values of: thickness ( $d$ ) and component concentrations in sol-gel  $\text{Si}_{1-x}\text{Ge}_x\text{O}_2$  films.

$T_{\text{ann}}(^{\circ}\text{C})$	$d(\text{nm})$	$\text{SiO}_2(\%)$	$\text{GeO}_2(\%)$	voids(%)	a-Ge(%)
550	112.9	94.50	5.40	0.10	0.00
800	101.0	94.63	4.95	0.08	0.34
950	98.8	98.17	1.62	0.21	0.00

As an important result of the SE investigation, we can conclude that an optimized moderate annealing is necessary to form Ge clusters embedded in oxide matrix.

#### 4. Conclusions

Sol-gel method was used to produce compact and adherent  $\text{Si}_{1-x}\text{Ge}_x\text{O}_2$  films. XTEM investigations performed on a sample annealed at  $850^\circ\text{C}$  have shown the presence in the oxide matrix of Ge-rich amorphous clusters of 5-10 nm in diameter. By analysis of SE data valuable information was obtained about the film composition and its evolution with the annealing. A significant formation of Ge clusters embedded in oxide was observed for moderate annealing at  $800^\circ\text{C}$ .

#### Acknowledgement

Work performed in part under CEEX programs, contracts No. 318/2006 and 13/2006.

#### References

- [1] S. Lombardo, B. De Salvo, C. Gerardi, T. Baron, *Microelectron. Eng.* **72**, 388 (2004).
- [2] P. W. Li, W. M. Liao, D. M. T. Kuo, S. W. Lin, P. S. Chen, S. C. Lu, M-J. Tsai, *Appl. Phys. Lett.* **85**, 1532 (2004).
- [3] H. K. Liou, P. Mei, U. Gennser, E. S. Yang, *Appl. Phys. Lett.* **59**, 1200 (1991).
- [4] M. Zacharias, J. Blbing, M. Liihmann, J. Christen, *Thin Solid Films* **278**, 32 (1996).
- [5] G. G. Qin, G. F. Bai, A. P. Li, S. Y. Ma, Y. K. Sun, B. R. Zhang, Z. C. Ma, W. H. Zong, *Thin Solid Films* 338-131 (1999).
- [6] H. Fukuda, T. Kobayashi, T. Endoh, S. Nomura, A. Sakai, Y. Ueda, *Appl. Surf. Sci.* **130-132**, 776 (1998).
- [7] A. V. Kolobov, A. A. Shklyayev, H. Oyanagi, P. Fons, S. Yamasaki, M. Ichikawa, *Appl. Phys. Lett.* **78**, 2563 (2001).
- [8] T. Stoica, E. Setter, *Nanotechnology* **17**, 4912 (2006).
- [9] Charles K.F. Ho, K. Pita, N. Q. Ngo, C. H. Kam, *Optics Express* **13**, 1049 (2005).
- [10] Charles K. F. Ho, Rajni, H. S. Djie, Kantisara Pita, Nam Quoc Ngo, T. Osipowicz, *Applied Optics* **46**, 4397 (2007).
- [11] T. F. Stoica, M. Gartner, T. Stoica, M. Losurdo, V. S. Teodorescu, M. G. Blanchin, M. Zaharescu, J. Optoelectron. *Adv. Mater.* **7(5)**, 2353 (2005).
- [12] G. A. N. Connell, R. J. Temkin, W. Paul, *Advances in Physics* **22(5)**, 643 (1973).

\*Corresponding author: tfstoica@infim.ro